ARTICLE IN PRESS

Theoretical and Applied Fracture Mechanics xxx (xxxx) xxx–xxx

Contents lists available at ScienceDirect

Theoretical and Applied Fracture Mechanics

journal homepage: www.elsevier.com/locate/tafmec

Prediction of fracture loci for $Cu_{47.5}Zr_{47.5}Al_5$

Jun Cao, Fuguo Li*, Xinkai Ma, Zhankun Sun

State Key Laboratory of Solidification Processing, School of Materials Science and Engineering, Northwestern Polytechnical University, Xi'an 710072, China

ARTICLE INFO

Keywords:
Fracture loci
Stress triaxiality
Bulk metallic glasses
Unified fracture criterion

ABSTRACT

Due to the difficulty of preparing large bulk metallic glasses (BMGs) samples and expensive cost, there are few reports for the fracture loci of BMGs. We proposed a method of plotting fracture loci in the stress and strain spaces to reveal the law of fracture loci of BMGs in the wide stress triaxiality range. The fracture loci of $Cu_{47.5}Zr_{47.5}Al_5$ in stress and strain spaces were investigated by using the proposed method. The different shapes of fracture loci were found under tensile and compressive stress states. Based on the fracture loci of $Cu_{47.5}Zr_{47.5}Al_5$, the plasticity of $Cu_{47.5}Zr_{47.5}Al_5$ is concentrated under special compressive states, such as uniaxial compression and balanced biaxial compression states. Additionally, stress triaxiality and Lode parameter largely affect the plasticity of BMGs.

1. Introduction

As the absence of dislocation-based plasticity in the disordered-lattice structure, most bulk metallic glasses (BMGs) exhibit that strengths and elastic limits are much higher than those of conventional crystalline alloys. In addition, BMGs exhibit good wear and corrosion resistance at room temperature [1,2], while the ductility is usually low [3,4]. The bulk glass formation in binary Cu-Zr alloys and in ternary Cu-Zr-Al alloys has triggered a lot of interest in glass-forming systems [5–9]. The plasticity change tendency in terms of changing composition in $(Cu_{50}Zr_{50})_{100-x}Al_x$ (x = 0–8 at.%) has been studied [10] and the results show that the plasticity of the BMGs is sensitive to the change of Al content. In addition, the plastic deformations with regard to Al percentage composition in $(Cu_{50}Zr_{50})_{100-x}Al_x$ exhibits significant different and a maximum plasticity of 16% is reached for $(Cu_{50}Zr_{50})_{95}Al_5$.

Efforts were made to investigate the fracture behavior of BMGs in the recent years [11–15]. A great number of evidences [16,17] show that the deformation of BMGs could be accomplished by the local arrangement of some atomic clusters which can provide the shear strain and the local arrangement of atoms often occurs at high stresses and energies. The most commonly used theoretical models are the free volume theory proposed by Spaepen [18] and the shear transformation zone (STZ) theory proposed by Argon [19], then subsequently improved by Langer et al. [17,20]. Schuh and Lund [21,22] used atomistic simulations to examine the deformation characteristics of STZs. They computed the yield surface of a metallic glass for biaxial loading and fitted better by Mohr-Coulomb criterion using empirical inter-atomic potentials. Song et al. [23] studied the fatigue endurance limit and crack growth behavior of a high toughness $Zr_{61}Ti_2Cu_{25}Al_{12}$ bulk metallic glasses. Zhang and Eckert [24] firstly proposed unified fracture criterion and then the fracture criterion was developed by Qu and Zhang [11]. In addition, Cao and Li [25] developed the fracture criterion based on strain energy density.

It is important to notice that the fracture loci in the wide stress triaxiality range are required in the design and application of BMGs. However, because of the difficulty in the manufacturing of BMGs and expensive cost in the lots of fracture experiments, there are few reports about the fracture loci for BMGs. Therefore, the aim of present study is to predict the fracture loci in the wide stress triaxiality ranges for BMGs. In this paper, the fracture loci of $Cu_{47.5}Zr_{47.5}Al_5$ under biaxial and triaxial states were systematically studied using unified fracture criterion. The different shapes of fracture loci under tensile and compressive stress states reflect different fracture mechanisms under the two states. In addition, the stress triaxiality and Lode parameter are found as two important influencing factors for the plasticity of BMGs.

2. Method

2.1. Proposed method to predict the fracture loci in stress and strain spaces

The unified fracture criterion [11] satisfactorily describe the fracture behavior of the BMGs, and the expression is

$$\tau^2 + \alpha^2\beta\sigma^2 = \tau_0^2 \tag{1}$$

where α is the ratio of critical shear fracture stress τ_0 to critical normal fracture stress σ_0, and β is a external parameter, which is 1 when $\sigma > 0$,

* Corresponding author.
E-mail address: fuguolx@nwpu.edu.cn (F. Li).

https://doi.org/10.1016/j.tafmec.2017.11.007
Received 12 May 2017; Received in revised form 21 November 2017; Accepted 28 November 2017

Please cite this article as: Cao, J., Theoretical and Applied Fracture Mechanics (2017), https://doi.org/10.1016/j.tafmec.2017.11.007

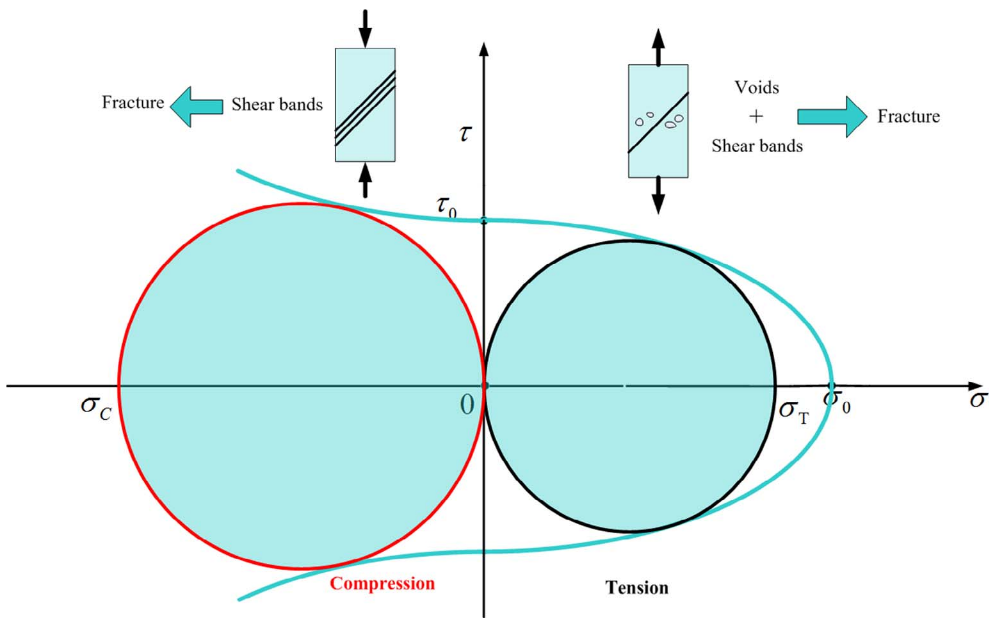

Fig. 1. Illustration of unified fracture criterion in the $\sigma-\tau$ coordinate.

is -0.5 when $\sigma < 0$ [11]. Fig. 1 illustrates the graphical representation of the unified fracture criterion. From Fig. 1, the critical fracture conditions under uniaxial tensile and compressive states can be predicted, as presented in Fig. 1. The different fracture mechanisms under tensile and compressive stress states are responsible for the difference of the fracture locus under the two stress states. The voids and shear bands under tensile stress state both play major role in the fracture process for BMGs, while only shear bands under compressive stress state can arouse fracture. In the compression state, the formation of voids is restrained, that is to say volume deformation does not promote the fracture process on this condition. Therefore, BMGs need more shear stress which is the driving force of shear deformation and then it can reach the fracture condition. Hence, more shear bands will be existed in the compression state due to shear deformation.

Fracture occurs when the largest Mohr's circle reaches the fracture locus of the unified fracture criterion in the $\sigma-\tau$ coordinate system. So the limit state equation can be obtained by combining Eq. (1) and the equation of largest Mohr's circle in a form of:

$$\alpha^2\beta\left(\frac{\sigma_1+\sigma_3}{2}\right)^2 + (1-\alpha^2\beta)\left(\frac{\sigma_1-\sigma_3}{2}\right)^2 = (1-\alpha^2\beta)\tau_0^2,\ \sigma_1 < \sigma_0 \tag{2}$$

where σ_1 and σ_3 are maximum and minimum principal stresses, respectively. The fracture loci in the two dimensional stress space of (σ_1,σ_2) can be plotted on the basis of Eq. (2). In addition, the fracture locus in stress space of $(\sigma_1,\sigma_2,\sigma_3)$ is transformed in the space of $(\bar{\sigma},R_\sigma,L)$ based on three expressions of principal stresses [26], which is derived in Appendix A, where $\bar{\sigma}$ is equivalent stress, R_σ is stress triaxiality and L is Lode parameter. Eq. (2) is easily expressed by R_σ, L and $\bar{\sigma}$ in a form of

$$\bar{\sigma}^2\left(\alpha^2\beta\left(R_\sigma-\frac{L}{3\sqrt{L^2+3}}\right)^2 + (1-\alpha^2\beta)\left(\frac{1}{\sqrt{L^2+3}}\right)^2\right) = (1-\alpha^2\beta)\tau_0^2 \tag{3}$$

The equivalent stress $\bar{\sigma}$ at a given stress state of (R_σ,L) is computed from the equivalent plastic strain $\bar{\varepsilon}^p$ with the true stress-strain curve, i.e. the phenomenological power law of $\bar{\sigma} = K^*(\bar{\varepsilon}^p)^{n^*}$. So the equivalent plastic strain $\bar{\varepsilon}^p$ is expressed as:

$$\bar{\varepsilon}^p = \left(\frac{(1-\alpha^2\beta)\tau_0^2}{(K^*)^2\left(\alpha^2\beta\left(R_\sigma-\frac{L}{3\sqrt{L^2+3}}\right)^2 + (1-\alpha^2\beta)\left(\frac{1}{\sqrt{L^2+3}}\right)^2\right)}\right)^{1/2n^*} \tag{4}$$

where K^* and n^* are just constitutive fitting parameters which are different from the strength coefficient K and strain hardening index n. K^* and n^* have no physical meaning for plastic deformation of metal, because there is almost no strain hardening for BMGs. Therefore, the fracture locus in the space of $(\bar{\varepsilon}^p,R_\sigma,L)$ can be mapped by using Eq. (4) and the fracture locus in the space of $(\bar{\varepsilon}^p,R_\sigma)$ under plane stress conditions can be mapped by applying the three expressions of principal stresses $\sigma_i = 0$, as illustrated in Appendix A. Based on the assumption of proportional straining, three expression principal strains are derived in Appendix A. The three branches of the fracture loci under plane stress conditions also can be mapped to the principal strain space of $(\varepsilon_1,\varepsilon_2)$ by using the definite relationship between R_σ and L with $\sigma_i = 0$. In addition, the stress and strain spaces of $(\sigma_1,\sigma_2,\sigma_3)$ and $(\varepsilon_1,\varepsilon_2,\varepsilon_3)$ with a cut-off stress triaxiality can be transformed into the deviatoric stress and strain space (S_1,S_2,S_3) and $(\varepsilon_1,\varepsilon_2',\varepsilon_3')$ in the segment a and A by using x-y coordinate of π-plane, as showed in Fig. 2. The transformed relations can be expressed as:

$$x = \begin{cases} \frac{\sqrt{3}}{2}(S_1-S_3) = \frac{\sqrt{2}}{2}(\sigma_1-\sigma_3) \\ \frac{\sqrt{3}}{2}(\varepsilon_1'-\varepsilon_3') = \frac{\sqrt{2}}{2}(\varepsilon_1-\varepsilon_3) \end{cases} \tag{5}$$

$$y = \begin{cases} \frac{1}{2}(2S_2-S_1-S_3) = \frac{\sqrt{6}}{6}(2\sigma_2-\sigma_1-\sigma_3) \\ \frac{1}{2}(2\varepsilon_2'-\varepsilon_1'-\varepsilon_3') = \frac{\sqrt{6}}{6}(2\varepsilon_2-\varepsilon_1-\varepsilon_3) \end{cases} \tag{6}$$

So the fracture loci in π-plane with stress and strain spaces can be plotted based on Eqs. (5) and (6), as can be seen in Appendix A. In Fig. 2, the stress and strain states in deviatoric stress and strain planes (π-planes) with variation of Lode parameter can be clearly observed. In the π-planes, there are six identical segments at every 60° which are symmetric. One identical segment is plotted then the other five identical segments can be all plotted in the stress and strain spaces (S_1,S_2,S_3) and $(\varepsilon_1',\varepsilon_2',\varepsilon_3')$. There are three kinds of strain states with Lode parameters are -1, 0 and 1 respectively, as the three Mohr's circles showed in the segment a of Fig. 2(a) and segment A of Fig. 2(b). In addition, the fracture surfaces in the spaces of (S_1,S_2,S_3,R_σ) and $(\varepsilon_1',\varepsilon_2',\varepsilon_3',R_\sigma)$ also can be mapped by changing the cut-off stress triaxiality value.

2.2. Materials constants of $Cu_{47.5}Zr_{47.5}Al_5$

Since the need of stress strain relation in the plotting fracture loci in strain spaces, the tensile and compressive engineering stress-strain curves of $Cu_{47.5}Zr_{47.5}Al_5$ and their converted true stress-strain curves